

Contents lists available at ScienceDirect

### Physica C: Superconductivity and its applications

journal homepage: www.elsevier.com/locate/physc





# Energy-scale considerations of unconventional superconductors—implications to condensation and pairing

Yasutomo J. Uemura

Physics Department, Columbia University, New York, NY 10027, USA

#### ARTICLE INFO

 $\it Keywords:$  High  $\it T_c$  superconductivity Muon spin relaxation Superfluid density

#### ABSTRACT

Discovery of high- $T_c$  cuprate superconductors (HTSC) in 1986 by Bednorz and Muller, followed by synthesis of  $A_3C_{60}$ , iron-pnictides/chalcogenides and other exotic superconducting (SC) systems, introduced unconventional superconductors (UCSC) having their mechanisms of condensation and/or pairing distinctly different from those of simpler metals which can be explained by BCS theory. This article will show how one can demonstrate their new mechanisms by examining correlations among key energy-scale parameters, including the transition temperature  $T_c$ , the superfluid density  $n_s/m^*$ , the effective Fermi energy  $\varepsilon_F$ , the excitation energy of the magnetic resonance mode (MRM), the onset temperatures of Nernst effect and light-induced transient superconductivity, and the spin fluctuation energy scale  $\hbar\omega_{sf}$ , and by resorting to analogy / comparisons with superfluid <sup>4</sup>He as a representative system undergoing Bose Einstein Condensation (BEC). We will propose a paring mechanism in HTSC based on resonance of spin ( $\hbar\omega_{sf}$ ) and charge ( $\varepsilon_F$ ) energy scales, and apply that concept for explaining unusual behaviors in the overdoped region. We will also discuss modifications of a simple BEC-BCS crossover picture to account for actual situations with additional effects of competing order and phase separation.

#### Chapter I. Correlations between $T_c$ vs. $n_s/m^*$ , and $T_c$ vs. $\varepsilon_F$

Soon after the discovery of HTSC systems [1], we started measurements of the muon spin relaxation rate  $\sigma$  by applying a transverse magnetic field of a few kG. In Type II superconductors the relaxation is caused by the inhomogeneity of the local field distribution due to the Abrikosov lattice of flux vortices, which is proportional to the inverse square of the magnetic field penetration depth  $\lambda$  as  $\sigma \propto 1/\lambda^2$ . In the clean limit, London equation leads to  $1/\lambda^2$  given by the superconducting (SC) carrier density  $n_s$  divided by the effective mass  $m^*$  as  $\sigma \propto 1/\lambda^2 \propto n_s/m^*$ . For convenience's sake,  $n_s/m^*$  is often denoted as the superfluid density  $\rho_s$ . By 1989 we accumulated MuSR results on various HTSC systems with different doping levels, and plotted  $\sigma(T\rightarrow 0)$  against  $T_c$  as shown in Fig. 1 [2]. This figure shows that  $T_c$  exhibits a nearly linear correlations with  $n_s/m^*$  in the underdoped region, with a universal slope common to the 214, 123 and tripe-layer HTSC systems. To appreciate additional information given by the absolute values of  $\rho_s$ , we converted the superfluid density  $n_s/m^*$  to an effective Fermi energy  $\varepsilon_F$  by noticing that Fermi energy is proportional to superfluid density in highly anisotropic 2-dimensional systems, while one can obtain  $\varepsilon_F$  by combining  $n_s/m^*$ with another parameter, such as the Sommerfelt constant, for isotropic 3-d systems. Fig. 2 shows our initial attempt published in 1991 [3] to classify various superconductors in a plot of  $T_c$  versus  $\varepsilon_F$  derived from the superfluid density.

Among various messages of these results, Fig. 3 illustrates some of the simpler implications. As shown in Fig. 3(a), superfluid in BCS condensation includes all the carriers of the Fermi sphere whose dissipation is prevented below  $T_c$  by the formation of the energy gap at the Fermi surface. As long as any small gap is formed, all the carriers participate in the superfluid in the ground state.  $T_c$  scales with the gap size which depends primarily on the size of pairing attractive interaction. Therefore, there is no immediate (zeroth order) correlation expected between  $T_c$  and the superfluid density. This is not compatible with the strong correlation between  $T_c$  and  $n_s/m^*$  found in Fig. 1. This feature was one of the earliest indications which suggested that HTSC systems may follow a mechanism distinctly different from BCS condensation. By combining independent information on  $m^*$  and the coherence length, the superfluid density results can also be used to estimate an overlap of pairs in real space. As shown in Fig. 3(b), only several pairs are overlapping with each other for HTSC systems showing the linear correlations in Fig. 1. This is the situation between the cases of BCS condensation with thousands of pairs overlapping and BEC condensation of superfluid <sup>4</sup>He with nearly independent bosons, while being impressively close to the latter.

E-mail address: yu2@columbia.edu.

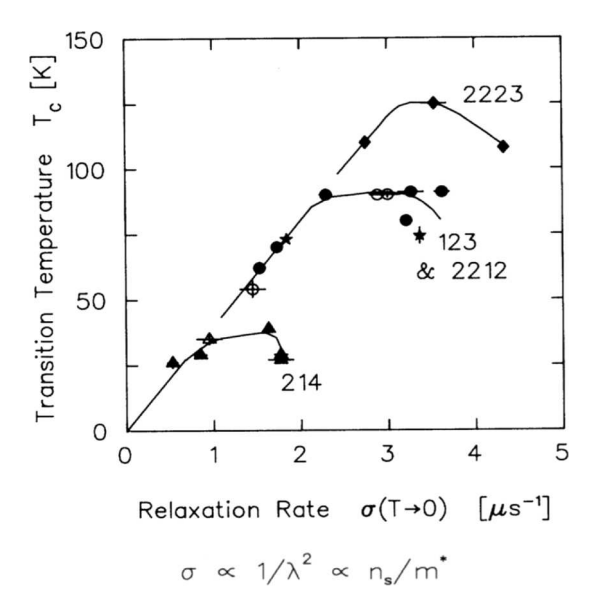


**Fig. 1.** Muon spin relaxation rate  $\sigma$  in transverse fields (a few kG) at T=2 K in sintered ceramic specimens of HTSC with various doping levels in a few different families plotted against the SC transition temperature  $T_c$ , initially published in 1989 [2].

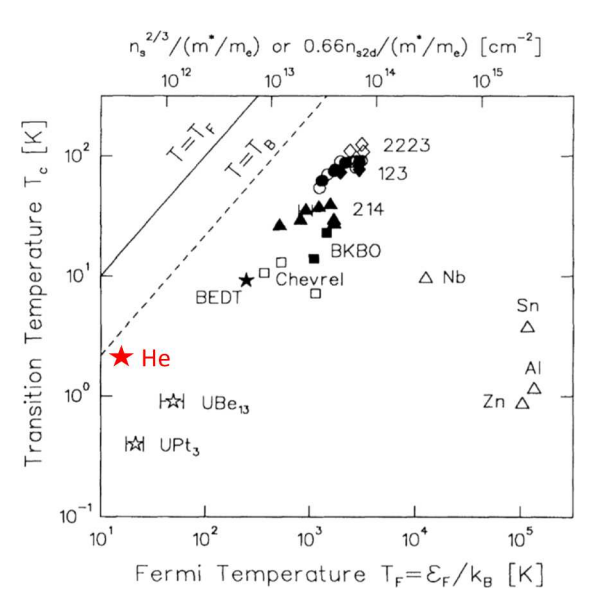


**Fig. 2.** The effective Fermi temperature derived from the superfluid density  $n_s/m^*$ , plotted against  $T_c$  in various UCSC systems, initially published in 1991 [3]. A point for superfluid <sup>4</sup>He, added for the present article, is shown by the red star symbol.

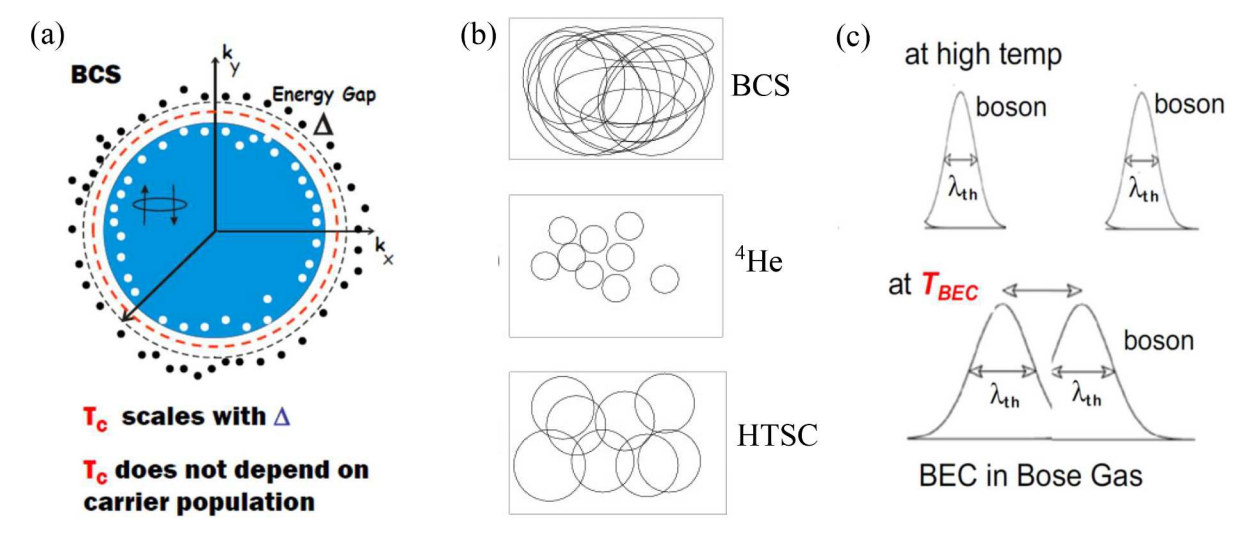


Fig. 3. Characteristic features of BCS and BEC condensations: (a) In BCS condensation magnitude  $\Delta$  of the SC energy gap around the Fermi sphere scales with  $T_c$  while all the carriers (blue region) join the superfluid density regardless of the gap size (red or black). (b) Overlap of bosonic pairs in real space at T→0. HTSC systems have only several pairs overlapping, close to BEC of superfluid <sup>4</sup>He. (c) Thermal wave length  $\lambda_{th}$  of a boson in an ideal Bose gas. BEC occurs when  $\lambda_{th}$  becomes comparable with the inter-boson distance.

In non-interacting Bose gas, bosons behave as classical particles at high temperatures as long as their thermal wave length  $\lambda_{th}$  is significantly shorter than the inter boson distance  $d_{boson}$ , as illustrated in Fig. 3 (c). With decreasing temperature  $\lambda_{th}$  becomes longer. When  $\lambda_{th}$  becomes comparable to  $d_{boson}$ , quantum phase coherence develops between adjacent bosons, and BEC takes place if there are no other preventive factors such as dimensionality and/or competing interaction. One can compare real systems with such idealized hypothetical Bose gas by assuming boson density to be  $n_s/2$  and the boson mass  $2m^*$  from Fig. 2. In such hypothetical situation, one would have expected BEC to occur at  $T_{BEC}$  shown by the broken line in Fig. 2. It is notable that actual  $T_c$  of HTSC system is reduced by about a factor 4–5 comparted to  $T_{BEC}$ , while the linear correlations in Figs. 1 and 2 are parallel to the behavior expected in non-interacting Bose gas. This feature, together with the real space situation in Fig. 3(b). suggests that condensation mechanism of HTSC systems is deeply related to BEC, but some serious revisions may

be required to account additional factors such as inter-boson interaction, spatial overlap, competing order and phase separation. Note that thermal pair-breaking excitations, which determines  $T_c$  in BCS condensation, cannot explain  $T_c$  of HTSC systems, especially in the underdoped region where  $T_c$  increases while the pseudo-gap energy decreases with increasing hole carrier doping.

### Chapter II. Magnetic resonance mode (MRM) and rotons: BEC with existence of competing order

In the case of superfluid  $^4$ He, the actual lambda point  $T_c=2.2$  K in ambient pressure is reduced from  $T_{BEC}\sim3.2$  K derived from the density and mass of He, as shown by the red symbol in Fig. 2. In 1970's Ruvalds theoretically showed that  $T_c$  of  $^4$ He can be calculated by considering inelastic thermal excitations of rotons [4]. Rotons represent short-range and temporal atomic correlations related to the competing HCP solid He,

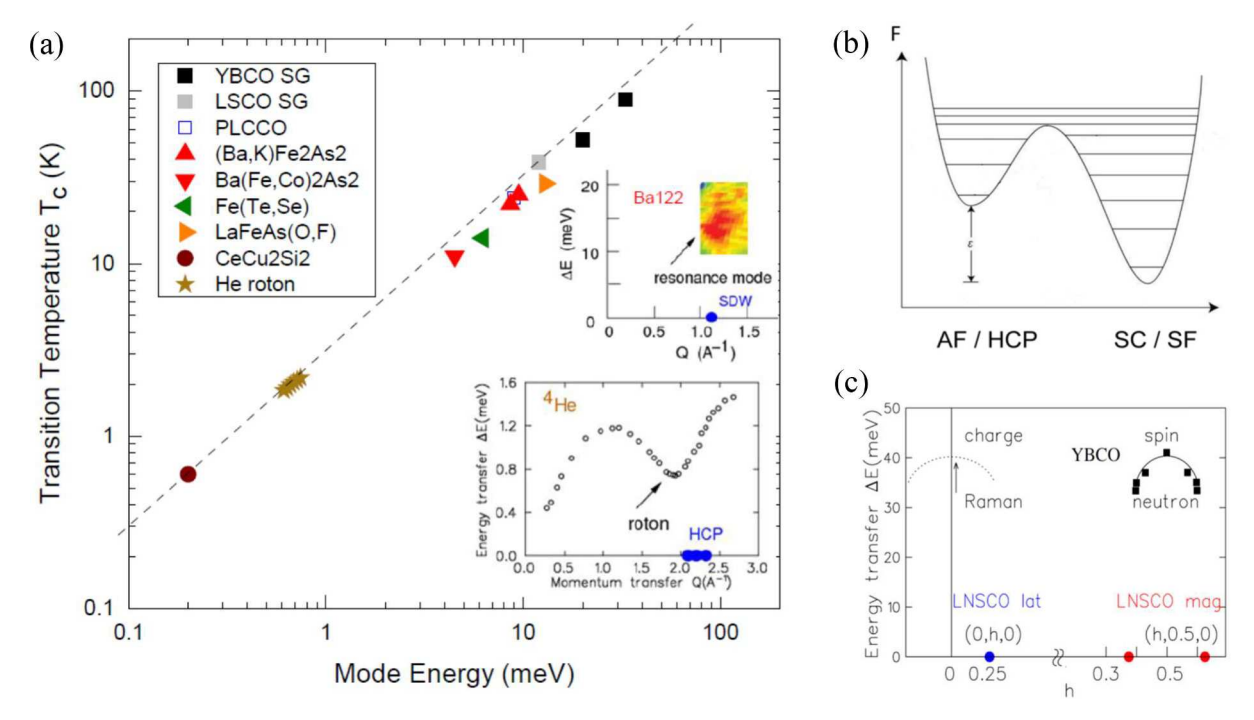


**Fig. 4.** Magnetic resonance mode (MRM) in UCSC and rotons in superfluid <sup>4</sup>He [7]. (a) Plot of the mode energy vs  $T_c$  with He results in ambient / applied pressure and spin-gap energy representing MRM in HTSC. (b) Competing orders in HTSC (SC vs AF) and in He (Super Fluid (SF) vs HCP solid). with a double-well free energy profile. (c) Proposed dispersion of the MRM with the spin branch near  $(\pi,\pi)$  and a twin charge branch near the zone center [5].

appearing as a soft phonon mode towards eminent HCP order near the Bragg point of solid He, as if a bubble of competing ordered state were floating in superfluid <sup>4</sup>He. By 2004 the present author realized [5] that: (i)  $T_c$  of the superfluid <sup>4</sup>He scales with the roton energy observed by neutron scattering [6] in ambient and applied pressure; and (ii)  $T_c$  of HTSC and various other UCSC scales with the excitation energy of the neutron magnetic resonance mode (MRM) with the ratio of mode energy vs  $T_c$  nearly identical to that of rotons in superfluid <sup>4</sup>He [7]. This situation is demonstrated in Fig. 4 [5,7]. The MRM represents inelastic spin excitations with the periodicity of competing spin-stripe / antiferromagnetic (AF) order in UCSC, as shown in the inset of Fig. 4(a) which illustrates the similarity of the MRM and rotons in <sup>4</sup>He. If we assume that the MRM represents a soft mode towards competing AF / spin-stripe order, and if its excitation contributes towards depletion of the SC condensates in HTSC and UCSC, then thermal excitations of the MRM can provide a mechanism for the 4-5 times reduction of  $T_c$  of these systems from  $T_{BEC}$ .

Both of the rotons and the MRM would have excitation energy corresponding to the free energy difference of the ground states of the competing superfluid/SC order and HCP solid/AFM-stripe order, as illustrated in Fig. 4(b). This picture with the double-well free energy profile is consistent with phase diagrams of several UCSC and <sup>4</sup>He, depicted in Fig. 5 [8], where the boundaries of the competing phases appear with first order phase transitions and/or phase separation. It is notable that the MRM is also observed by a charge probe Raman scattering [9] at the energy transfer corresponding one to one with the neutron spin excitation energy. For the case of spin-alone excitation detected by Raman, we expect Raman energy having twice the spin energy in the "two magnon Raman" process. The one-to-one Raman energy suggests existence of charge mode near the zone center with the same energy as spin mode near the momentum transfer of the AF correlations, as illustrated in Fig. 4(c) [5]. Such a spin-charge twin mode can be expected when spin and charge correlations are coupled very strongly, leading to formation of dynamic spin-charge stripes. A direct involvement of the charge sector can explain why thermal MRM excitations would deplete the SC charge condensate in HTSC systems, and

thus determine  $T_c$ . The inelastic charge branch may become detectable in Resonant Inelastic X-ray Scattering (RIXS) studies on HTSC systems with improved energy resolutions in the future.

#### Chapter III. Photo-induced transient superconductivity and the Nernst effect: manifestations of local phase coherence among preformed pairs

Ong and co-workers [10,11] observed vortex Nernst effect well above  $T_c$  in the underdoped region of HTSC systems in 2000–2010. The onset temperature  $T_{nern}$  of the Nernst effect and that of the diamagnetic susceptibility [12] in the 214 HTSC systems follow the  $T_{BEC}$  line in the highly underdoped region [5,7], as shown in Fig. 6(a) and (b) [7]. In the phase diagram of the (La,Sr)<sub>2</sub>CuO<sub>4</sub> (LSCO) system (Fig. 6(b)), bosonic (2e) pairs are gradually formed with decreasing temperature below the pseudogap temperature  $T^*$  derived from the susceptibility ( $T^*_{chi}$ ) and conductivity  $(T^*_{rho})$ .  $T^*$  represents the magnitude of attractive interaction between two unpaired fermion charges, in a "two-body" physics. In the highly underdoped region, with decreasing temperature below  $T^*$ , most of the normal-state carriers are paired into bosons at or above  $T_{BEC}$  $\sim 4-5 T_c$ . Then a local phase coherence among adjacent bosons will develop around  $T_{BEC}$  as illustrated in Fig. 3(c). This is a "many-body" process related to the boson density and mass. Due to competing AF order and thermal MRM excitations, however, global phase coherence for the SC order develops at  $T_c$ , well below  $T_{BEC}$ . With increasing hole doping towards the "optimal  $T_c$ " region,  $T_{nern}$  exhibits a marked departure from  $T_{BEC}$  derived from the superfluid density at  $T\rightarrow 0$ . The vortex Nernst effect is associated with local phase coherence among adjacent preformed bosons in the normal state. Since  $T^*$  is rapidly reduced with increasing doping, the density of preformed pairs would exhibit a saturation and suppression, as shown in Fig. 6(b) by the trajectory of  $T_{nern}$ . In contrast,  $T_{BEC}$  exhibits a monotonic increase up to the optimal doping, since  $T_{BEC}$  is derived from the superfluid density at  $T \rightarrow 0$ , which includes both paired (2e) and unpaired (e) carriers in the normal state. In the region between  $T_{nern}$  and  $T_c$ , a local and dynamic phase coherence is achieved among preformed bosons, yet without global phase

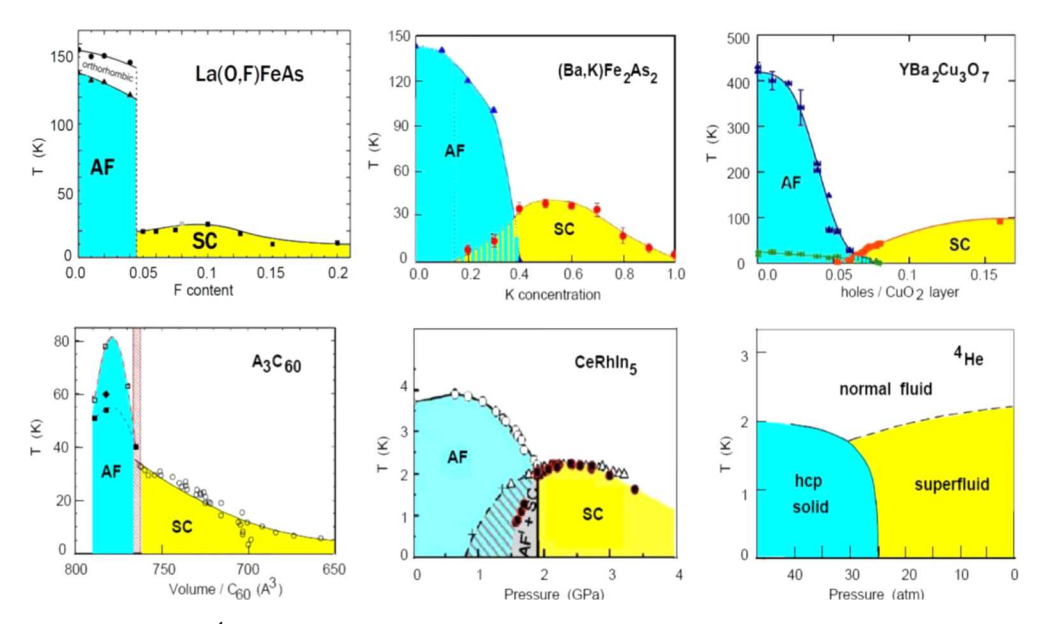


Fig. 5. Phase diagrams of several UCSC and <sup>4</sup>He systems [8]. In UCSC, the SC phase (yellow) appears adjacent to the competing AF phase (blue), while superfluid phase adjacent to the HCP solid phase in <sup>4</sup>He. Boundary of these competing phases appears with first order transitions and/or phase separation, consistent with the double-well free energy.

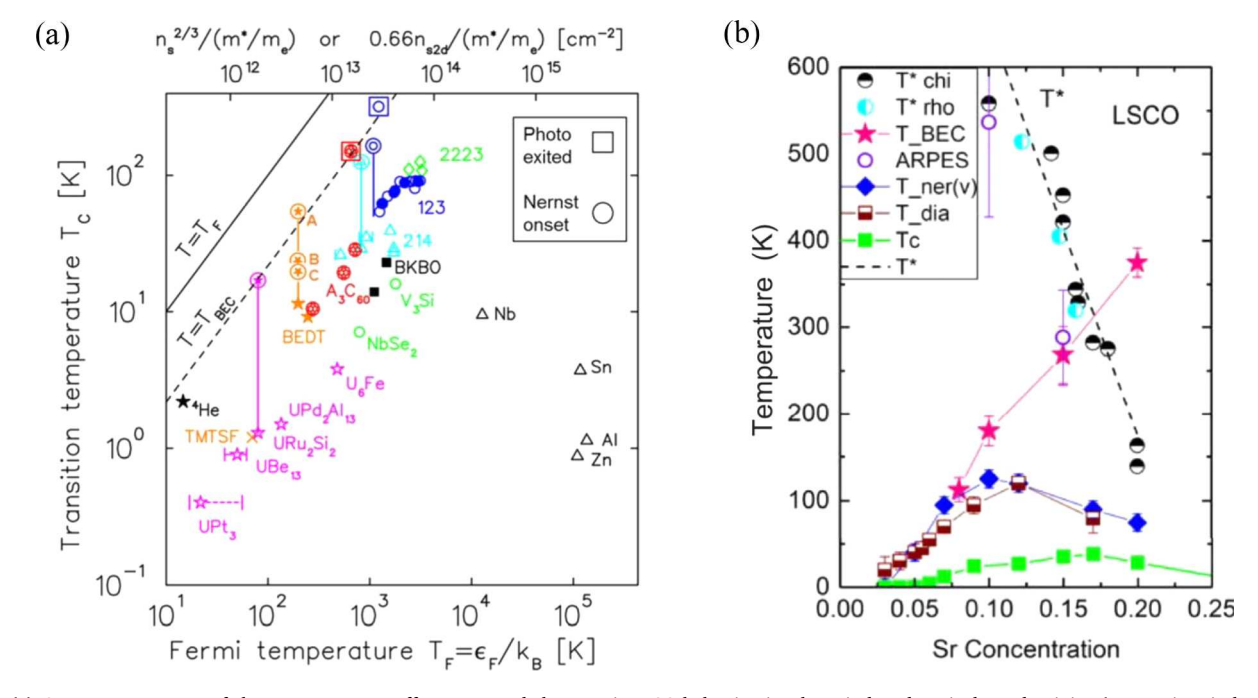
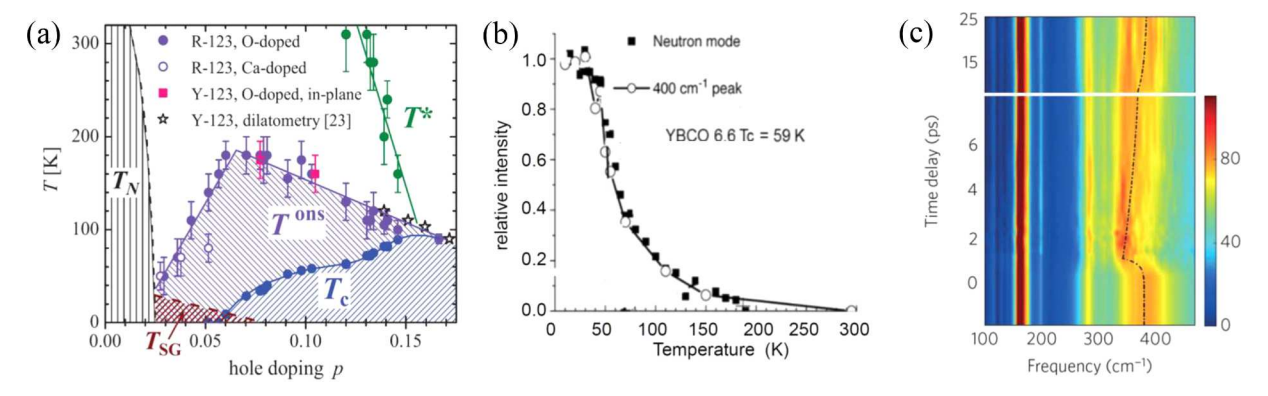


Fig. 6. (a) Onset temperature of the vortex Nernst effect  $T_{nem}$  and the transient SC behavior in photo-induced optical conductivity (composite circle / square symbols) of underdoped HTSC,  $K_3C_{60}$ , BEDT, and  $URu_2Si_2$  plotted vs effective Fermi temperature derived from the equilibrium and transient superfluid density in MuSR and ultra-fast optical studies [7]. The points lie close to the hypothetical  $T_{BEC}$  (broken line) at which a phase coherence is expected to develop among adjacent preformed bosons and the SC order would occur if adverse effects from competing order and/or dimensionality can be removed. (b) Phase diagram of LSCO systems [7] with the onset temperatures of pseudo gap  $T^*$ , Nernst effect and diamagnetic susceptibility, and  $T_{BEC}$  derived from the  $T \rightarrow 0$  superfluid density, compared with actual  $T_c$ .

coherence. As shown in Fig. 6(a) [7],  $T_{nem}$  was observed near  $T_{BEC}$  also in the underdoped YBCO [13], organic BEDT system close to the boundary to the AF state [14], and even in URu<sub>2</sub>Si<sub>2</sub> at the onset of the "hidden order" [15].

Since about a decade ago, Cavalleri and co-workers have reported signatures of transient SC behavior in ultrafast time-resolved studies of optical conductivity after exciting HTSC [16–18],  $K_3C_{60}$  [19,20] and BEDT [21] systems with high-intensity laser pulses. In measurements in equilibrium state without laser, Drude response of optical conductivity

in the normal state is suppressed in the SC state, forming a  $\delta$  function at  $\omega=0$ . This allows an estimate of the superfluid density from the missing Drude spectral weight. In ultrafast studies, photo excitations led to transient responses with missing Drude weight appearing at temperatures well above equilibrium  $T_c.$  The present author obtained the transient superfluid density and the onset temperature of the transient Drude suppression from the published photo-excited results, and plotted the corresponding values in Fig. 6(a). The points with photo excitations from underdoped LSCO, YBCO and  $K_3C_{60}$  systems come close to the  $T_{BEC}$ 



**Fig. 7.** Behaviors of optical 400 cm<sup>-1</sup> mode responses in YBCO. (a) Onset temperature  $T^{ons}$  of this mode in equilibrium optical studies by Bernhard et al. [22]. (b) Identical intensity vs T profiles of the optical mode and MRM in YBCO 6.6 in the equilibrium state [23]. (c) Time evolution of the transient optical responses after laser excitation at t = 0, observed in YBCO 6.5, showing correspondence of the optical mode and the transient SC behavior [17].

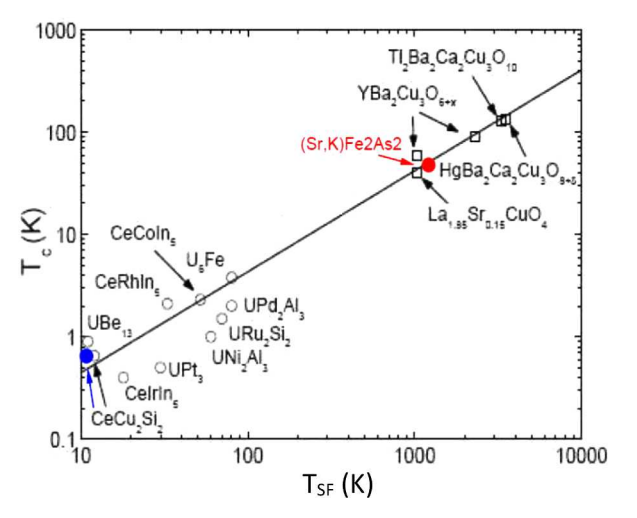


**Fig. 8.** Plot of  $T_c$  vs the spin fluctuation energy  $T_{SF}$  in various UCSC generated by Moriya and Ueda [24,25] with  $T_{SF}$  derived from neutron data of spin wave and paramagnetic fluctuations at the zone boundary and/or theoretical modeling based on the Moriya theory of itinerant magnets.

line, similarly to the case of the Nernst onset temperature. After seeing the results in these systems, the present author encouraged Cavalleri to measure photo-excited responses in BEDT systems, which was indeed found [21] to give the point in Fig. 6(a) lying close to the Nernst results.

In  $La_{2-x}Ba_xCuO_4$  (LBCO) with x = 0.115, photo excitation caused transient melting of long-range spin-charge stripe order while promoting SC responses [16]. In equilibrium optical conductivity studies, Berhhard and co-workers [22] reported that the 400 cm<sup>-1</sup> response (400 cm<sup>-1</sup> mode) appears in the region similar to that of the vortex Nernst effect in YBCO systems, as shown in Fig. 7(a). Prior to this, Timusk and Homes [23] noticed in YBCO 6.6 that the neutron MRM and the optical 400 cm<sup>-1</sup> mode exhibit the same temperature dependence of their intensities (Fig. 7(b)). In the ultrafast studies of YBCO 6.5, a transient suppression of the 400 cm<sup>-1</sup> mode was observed after laser irradiation [17] as shown in Fig. 7(c), while transient SC responses are observed together with increased transient  $T_c$ . These results suggest that: (i) the laser excitation can temporarily change the balance between AF-stripe and SC interaction in favor of SC; and (ii) the MRM and the 400 cm<sup>-1</sup> mode are both tied to the AF-stripe interaction. Laser irradiations suppressed static long-range AF-stripe order in LBCO while eliminated MRM and optical "inelastic modes" in YBCO, both resulting in promotion of the SC order. The 400 cm<sup>-1</sup> mode may be related to the charge branch of the MRM dispersion [5] illustrated in Fig. 4(c).

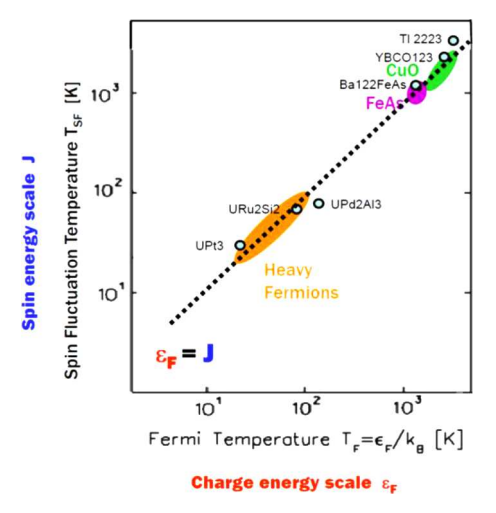


**Fig. 9.** Plot of  $T_{SF}$  from Fig. 8 vs the effective Fermi energy  $T_F$  from Figs. 2 and 6 in HTSC and FeAs systems at the optimal doping region and some heavy fermion SC systems generated by Uemura [26], which suggests nearly identical spin and charge energy scales.

# Chapter IV. Optimal doping region characterized by the charge spin resonance

In BCS theory attractive interaction via lattice distortion is formally described as the result of phonon exchange, which makes  $T_c$  proportional to the Debye frequency. In the case of coupling mediated by spin fluctuations, which is a quite likely scenario for HTSC, heavy fermion, and a few other UCSC systems, the energy scale of spin fluctuations  $\hbar\omega_{SF}$ would play a role of the Debye frequency if those systems follow BCS condensation. This consideration motivated Moriya and Ueda [24,25] to generate a plot of  $T_c$  vs  $\hbar\omega_{SF}$  including the results for many UCSC systems, as shown in Fig. 8. Experimentally  $\hbar\omega_{SF}$  is estimated often by the energy of magnons and/or paramagnetic spin fluctuations observed at the AF Zone boundary, while the results for some of the systems in Fig. 8 were obtained via theoretical modeling of parameters based on Moriya's theory for magnetism in itinerant electron systems. We see signatures of nearly linear  $T_c$  vs  $\hbar\omega_{SF}$  correlations in Fig. 8, which looks alike with the  $T_c$  vs  $\varepsilon_F$  plot in Figs. 2 and 6(a). This is due to the fact that the charge ( $\varepsilon_F$ ) and spin  $(\hbar\omega_{SF})$  energy scales are very close in values in some prototypical UCSC systems, as shown more explicitly in the  $\varepsilon_F$  vs  $\hbar\omega_{SF}$  plot in Fig. 9 [26]. In optimally doped HTSC systems, for example, these parameters have the values of about 2000-3000 K. To the present author, this special feature seems not to be due to simple accidental coincidences. In contrast, it may be an essential property which maximizes

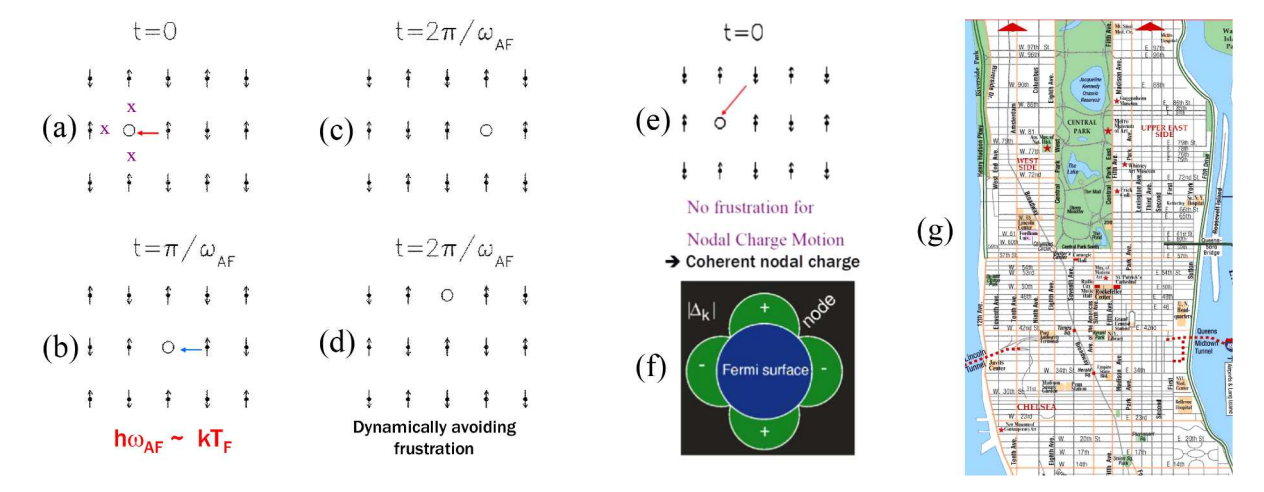


**Fig. 10.** Motion of a charge with energy  $\varepsilon$  in a resonance with AF spin fluctuations  $\hbar\omega_{AF}$  on a square lattice Heisemberg AF model: (left) (a) For  $\hbar\omega_{AF} << \varepsilon$ , a hopping to tetragonal (antinodal) directions generates additional frustrating bonds: (b) for  $\hbar\omega_{AF} \sim \varepsilon$ , the frustration can be avoided dynamically; (c) this can occur coherently towards the same direction or (d) incoherently towards orthogonal direction; (e) direct hopping to diagonal (nodal) direction does not generate additional frustrated bonds. (f) d-wave SC gaps on the CuO<sub>2</sub> planes of HTSC; (g) a map of streets and avenues in New York City, where traffic light alternation is synchronized with the speed of moving cars on major vertical avenues. [5,27].

### $T_c$ in the "dome-like" phase diagram as a function of doping.

Possible benefit of the resonating charge and spin energies can be considered for a charge motion of a nearly half-filled band with AF Heisenberg interaction on a 2-dimensional square lattice, shown in Fig. 10 [5,27]. When the charge motion is much slower than the spin fluctuations, the background AF lattice looks static to the charge, and a hopping of a hole to the nearest neighbor site towards the direction parallel to the tetragonal lattice (antinodal direction) would generate additional frustrated bonds. This feature would make the AF correlations hostile against the charge motion. The development of this frustration can be avoided for a special case where a spin fluctuation alternates the spin direction of the background lattice in synchronization with the charge motion, which can be expected for  $\varepsilon_F \sim \hbar \omega_{SF}$ . This hopping motion can take place coherently as illustrated in Fig. 10, and charges can dynamically avoid frustration due to the AF interaction and lattice. For a hopping towards diagonal (nodal) direction on the same spin sub-lattice, however, a charge motion does not change the frustration energy. This may be the origin of the difference between less coherent and nearly localized antinodal charges and more coherent nodal charges on the CuO2 planes of HTSC systems. This spin-charge resonance resembles a smooth motion of cars aided by a traffic-light synchronization on major avenues of New York City [27]. If this resonance occurs for two hole charges in a cooperative way, that could provide an attractive interaction for the formation of a bosonic pair.

## Chapter V: Anomalous coexistence of paired and unpaired charges in the overdoped HTSC

In 1993, MuSR studies of HTSC systems were extended from underto optimal doping region to overdoped Tl2201 [28,29]. As shown by Fig. 11, the superfluid density at  $T\rightarrow 0$  was found to decrease with increasing overdoping, crudely scaling the reduction of  $T_c$ , instead of following the increase of normal-state carrier density. This implies that the ground state is characterized by coexistence of paired superconducting charges  $(n_s)$  and unpaired remaining fermion charges  $(n_n)$ . Support to this picture was also found in non-zero remaining response of T-linear specific heat and in-gap optical conductivity well below  $T_c$ , as well as the reduction of the specific heat jump  $\Delta C/T$  at  $T_c$  with increasing overdoping (decreasing  $T_c$ ) [5]. Similar anomalous behavior in the overdoped HTSC was subsequently found in bulk samples of CaLaBa-LaCuO [30] and thin films of LSCO [31]. A possibility of microscopic phase separation was proposed [32] to account for this behavior, while

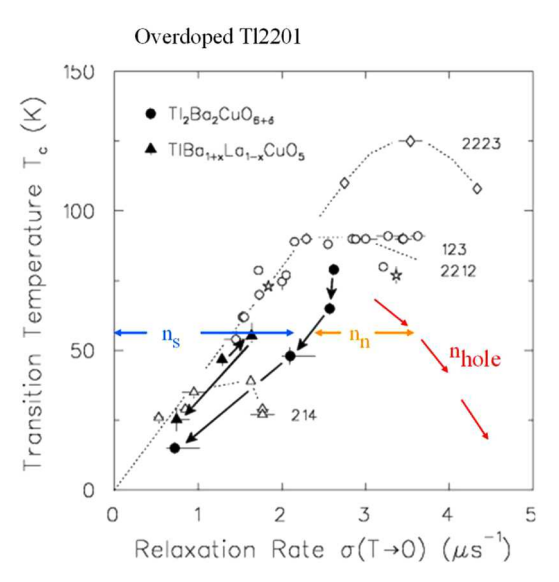


Fig. 11. MuSR results of  $\sigma \propto n_s/m^*$  in overdoped Tl2201 systems [28], where the superfluid density at  $T{\to}0$  decreases with overdoping, despite increase of the normal carrier density, suggesting paired carriers with density  $n_s$  and remaining unpaired carriers with  $n_n$  in the ground state.

signatures of spatial inhomogeneity was observed by neutron scattering on bulk and STM on thin film specimens of overdoped LSCO [33]. In the normal state above  $T_c$ , T-linear "Planckian" resistivity responses have been observed in optimal to overdoped HTSC systems, and connection was suggested between the charges forming the superfluid part in the overdoped HTSC below  $T_c$  and charges responsible for the Planckian behavior above  $T_c$  [34].

The spin–charge resonance picture in the previous chapter might suggest a possible origin of these anomalous behaviors in the overdoped region. For the spin-charge resonance, a carrier with energy  $\varepsilon$  requires to meet with a companion spin fluctuation of the same energy. In the underdoped region, where  $\varepsilon < \hbar \omega_{SF}$ , all the charges can find the spin fluctuation partner, and thus participate in the superfluid. This is possible only up to the optimal doping region where  $\varepsilon_F \sim \hbar \omega_{SF}$ . As illustrated in Fig. 12, only a fraction of charges can have the spin fluctuation partner in the overdoped region where charge energy exceeds  $\hbar \omega_{SF}$ . In addition, energy and/or spectral weight of spin fluctuations

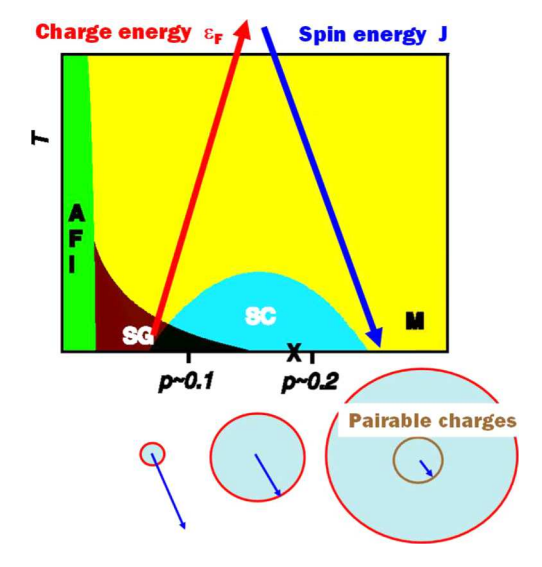


Fig. 12. Situation expected if charge carriers can form SC pairs only when a companion spin fluctuation exists with the charge–spin resonance situation. Beyond the optimal doping occurring at  $\hbar\omega_{AF}\sim\varepsilon_{F}$ , number of "pairable charges dressed with the spin-charge resonance" would decrease with further overdoping. This may explain Fig. 11.

may decrease with increasing doping which would gradually destroy the background AF lattice with frustration and percolation. This would result in coexistence of charges with and without spin fluctuation partners, which would form paired boson and unpaired fermion charges coexisting in the ground state of the overdoped HTSC.

### Chapter VI: Additional remarks on MRM, BEC-BCS crossover, and superfluid he films

Thin films of superfluid <sup>4</sup>He also provide additional insights. As shown in Fig. 13(a) [5],  $T_c$  is proportional to the superfluid density, having the ratio consistent with the universal value  $T_c/T_F = 1/8$  predicted by the Kosterlitz–Thouless (KT) theory, in thin films of superfluid

<sup>4</sup>He adsorbed on uniform Mylar film [35], porous Vycor glass [36], and <sup>4</sup>He-<sup>3</sup>He mixture adsorbed on fine powders [37]. Here, we do not see the effect of competing order via roton excitations. Roton energy in superfluid He films remains nearly unchanged from that in bulk superfluid <sup>4</sup>He [38,39] while  $T_c$  is reduced significantly, as shown in Fig. 13(b) for a film with  $T_c \sim 1$  K [39] compared with bulk superfluid <sup>4</sup>He with  $T_c = 2.2$ K [40] in Fig. 13(c). For films with very thin coverage and low  $T_c$ , interatomic distance becomes longer than that of solid He. With increasing temperature from the ground state, the KT transition occurs well before the roton-like excitations (if ever existed) play any important thermodynamic roles in thin He films with highly reduced  $T_c$ . This feature can also be seen in their nearly T-independent superfluid density below  $T_c$  [35]. In this sense, Fig. 13(a) illustrates examples of boson systems without the effects of competing order. It is impressive that achievement of global phase coherence is quite robust against strong disorder in porous media and even against coexisting uncondensed fermions of <sup>3</sup>He. These are similar to features observed in Zn-doped YBCO cuprates in a "Swiss cheese" like situation [5,41] and in overdoped HTSC in coexistence of bosons and fermions in the ground state.

In conferences held in 1994 [42,43], the present author proposed to apply a simple BEC-BCS crossover picture shown in Fig. 14(a) to HTSC, with a remark that the optimal region may be determined via a comparison of  $\varepsilon_F$  and the pair-mediating boson energy  $\hbar\omega_B$  ( $\hbar\omega_{SF}$  for a spin-mediating pairing), separating the underdoped region with non-retarded and the overdoped region with retarded interaction. This indeed turns out to be the case in actual HTSC systems as described in Chap. IV. However, subsequent considerations for the effect of competing order led to modification of this picture into the one shown in Fig. 14(b), where the dynamic local and static global phase coherences develop at separate temperatures, respectively, at  $T_{LPC}$  and  $T_c$ . Although the overdoped region of HTSC is often considered as a simple Fermi liquid following BCS condensation, the results in Chap. V indicate that only a part of total carriers participate in superfluid, which is clearly different from the situation in BCS theory illustrated in Fig. 3(a).  $T_c$ seems to be determined still by the superfluid density in the overdoped region, distinctly different from ordinary BCS condensation. Thus, the BEC-BCS crossover picture requires serious improvements in the "BCS side" when applied to actual HTSC and UCSC systems.

In BCS theory where the normal state consists of unpaired fermion (e) charges, the thermal excitation which depletes the SC condensate

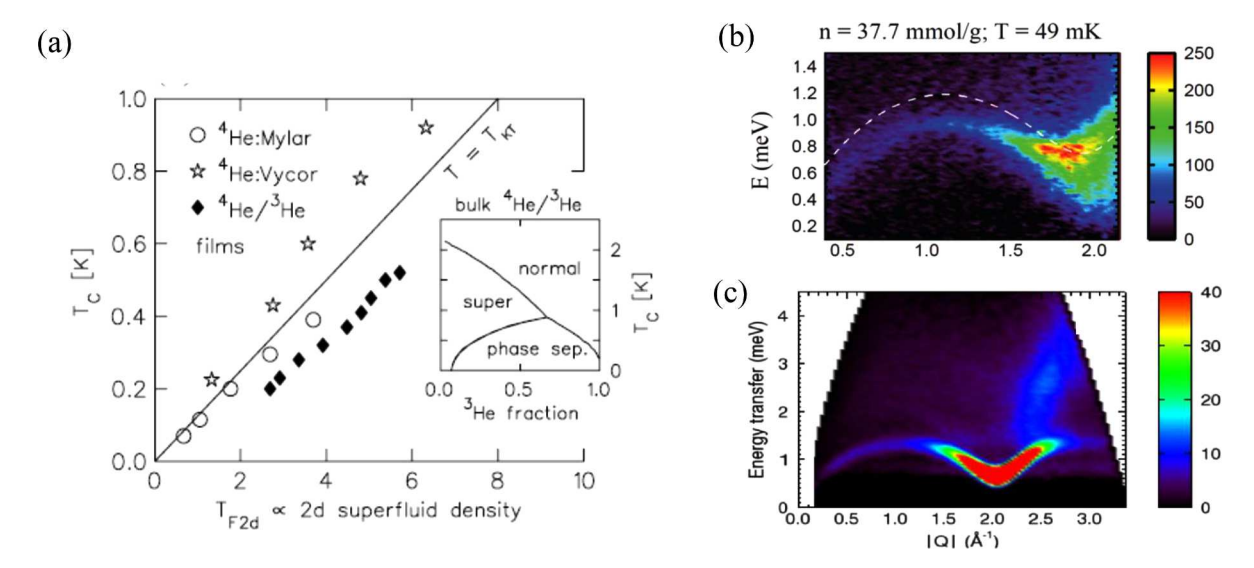


Fig. 13. Behavior of thin films of superfluid  $^4$ He. (a) Dependence of the superfluid  $^4$ C on the 2-dimensioal superfluid density [5], determined by torsion oscillators on He adsorbed on a smooth Mylar substrate [35], porous Vycor glass [36] and  $^4$ He/ $^3$ He mixture on fine powders [37], following predictions of Kosterlitz–Thouless theory  $T_c = T_{\rm F2d}/8$  (solid line). (b) inelastic neutron profiles of rotons from He films with  $T_c \sim 1.1$  K [39] and (c) from bulk He [40], both at  $T_c < T_c$ . Roton energy is not affected while  $T_c$  is reduced by a factor 2 in the film of (b).

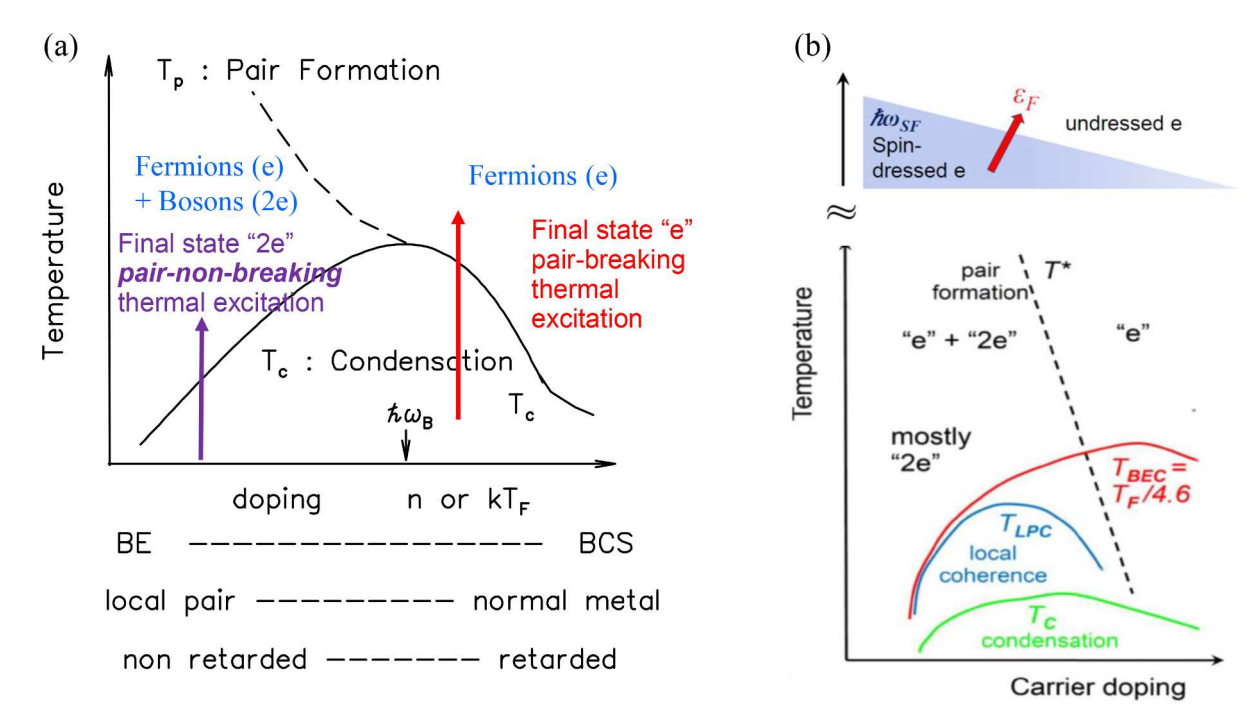


Fig. 14. (left) (a) BEC BCS crossover picture proposed in 1994 by the present author [42,43] to map to the situation of HTSC. Optimal  $T_c$  region was assumed to occur where the pair-mediating fluctuation (boson) energy  $\hbar\omega_B$  becomes comparable to the effective Fermi energy  $kT_F$ . This turns out to be indeed the case as shown in Fig. 9. Also shown are pair-non-breaking thermal excitations in the strongly underdoped region and pair-breaking excitations in the optimal and overdoped regions which would deplete the SC condensate and determine  $T_c$ . The MRM would include an additive sum of these two types of excitations [7]. (right) (b) phase diagram of HTSC systems which has the region of dynamic local phase coherence between  $T_{LPC}$  and  $T_c$  due to the effect of competing AF interaction suppressing the SC  $T_c$ . Spin fluctuation energy scale  $\hbar\omega_{SF}$  extending up to  $T \sim 2000$ –3000 K is shown by the blue shade, where the color gradation expresses decreasing spectral weight with charge doping. When sufficient spin fluctuations are available at  $\varepsilon < \hbar\omega_{SF}$ , a fermion charge (e) will be dressed by the spin fluctuations via the resonant spin–charge coupling illustrated in Fig. 10.

comes from the pair-breaking excitation across the energy gap. In the strongly underdoped region of HTSC, where normal state charges above  $T_c$  are mostly pre-formed (2e) bosons, pair-non-breaking thermal excitations should be the primary process for the condensate depletion, as illustrated in Fig. 14(a). The MRM is an excellent candidate for this excitation. With increasing hole doping towards optimal-doping, the normal state would become a mixture of paired (2e) and unpaired (e) charges, since the pair-formation energy  $T^*$  rapidly approaches  $T_c$ . Accordingly, the condensate-depleting excitations should become an additive mixture of the pair-non-breaking and pair-braking processes to account for the final state above  $T_c$ , and the MRM should also follow this behavior. In the optimal region where most of the normal-state charges are fermions, the MRM acquires characters of pair-breaking excitation across the energy gap of d-wave SC paring.

The charge motion accompanied by spin fluctuations in Chaps. IV and V may be described by using a concept of a composite fermion dressed by a boson representing spin interactions. The conceptual HTSC phase diagram in Fig. 14(b) also includes the possible effect of this dressing of a fermion charge due to the resonant spin-charge coupling. Inelastic x-ray and neutron studies in the overdoped LSCO [44] suggest that the spin fluctuation energy scale does not change much with doping, while we expect that the spectral weight will be reduced, as illustrated by the color gradient in Fig. 14(b). Then, the number of the "spin dressed" fermion charges will rapidly decrease with increasing overdoping. The spin-dressed fermion charges may also be related to the "Planckian" T-linear resistivity of HTSC systems. Observation of the Planckian behavior up to very high temperatures may be related to the high energy scale of the spin fluctuations extending up to  $\sim 2000$  K in HTSC systems. Hopefully, further energy-scale phenomenology, modeling with numerical simulations, and experimental verification of proposed conjectures will lead to ultimate understandings of condensation and pairing mechanisms of HTSC and UCSC systems.

#### **Declaration of Competing Interest**

The authors declare that they have no known competing financial interests or personal relationships that could have appeared to influence the work reported in this paper.

#### Data availability

Data will be made available on request.

#### Acknowledgment

The author would like to thank Karl Alex Mueller for his contributions in discoveries of HTSC systems and his open-minded interest in various different scenarios to explain HTSC; Graeme Luke, Kenji Kojima, Shin-ichi Uchida, and many other colleagues for collaboration in MuSR studies on UCSC accumulated since 1987; Hugo Keller and Andrea Cavalleri for useful discussions; Antonio Bianconi for organizing many informative meetings on HTSC and UCSC; and US NSF DMR 2104661 and Friends of U. Tokyo Inc. (FUTI) for financial support.

### References

- [1] J.G. Bednorz, K.A. Müller, Possible high T<sub>c</sub> superconductivity in the Ba–La–Cu–O system, Z. Phys. B64 (1986) 189.
- [2] Y.J. Uemura, G.M. Luke, B.J. Sternlieb, J.H. Brewer, J.F. Carolan, W.N. Hardy, R. Kadono, J.R. Kempton, R.F. Kiefl, S.R. Kreitzman, P. Mulhern, T.M. Riseman, D. Ll. Williams, B.X. Yang, S. Uchida, H. Takagi, J. Goparakrishnan, A.W. Sleight, M. A. Subramanian, C.L. Chien, M.Z. Cieplak, Gang Xiao, V.Y. Lee, B.W. Statt, C. E. Stronach, W.J. Kossler, X.H. Yu, Universal correlations between Tc and ns/m\* (carrier density over effective mass) in high-Tc cuprate superconductors, Phys. Rev. Lett. 62 (1989) 2317.
- [3] Y.J. Uemura, L.P. Le, G.M. Luke, B.J. Sternlieb, W.D. Wu, J.H. Brewer, T. M. Riseman, C.L. Seaman, M.B. Maple, M. Ishikawa, D.G. Hinks, J.D. Jorgensen,

- G. Saito, H. Yamochi, Basic similarities among cuprate, bismuthate, organic, chevrel phase, and heavy-fermion superconductors shown by penetration depth measurements, Phys. Rev. Lett. 66 (1991) 2665.
- [4] J. Ruvalds, Interacting rotons and superfluidity in liquid helium, Phys. Rev. Lett. 27 (1971) 1769.
- [5] Y.J. Uemura, Condensation, excitation, pairing, and superfluid density in high-Tc superconductors: the magnetic resonance mode as a roton analogue and a possible spin-mediated pairing, J. Phys.: Condens. Matter 16 (2004) S4515.
- [6] O.W. Dietrich, E.H. Graf, C.H. Huang, L. Passell, Neutron scattering by rotons in liquid helium, Phys. Rev. A 5 (1972) 1377.
- [7] Y.J. Uemura, Dynamic superconductivity responses in photoexcited optical conductivity and Nernst effect, Phys. Rev. Mater. 3 (2019), 104801.
- [8] Y.J. Uemura, Superconductivity: exotic commonalities in phase and mode, Nat. Mater. 8 (2009) 235.
- [9] Y. Gallais, A. Sacuto, P. Bourges, Y. Sidis, A. Forget, D. Colson, Evidence for two distinct energy scales in the Raman spectra of YBa<sub>2</sub>(Cu<sub>1-x</sub> Ni<sub>x</sub>)<sub>3</sub>O<sub>6.95</sub>, Phys. Rev. Lett. 88 (2002), 177401.
- [10] Z.A. Xu, N.P. Ong, Y. Wang, T. Kakeshita, S. Uchida, Vortex-like excitations and the onset of superconducting phase fluctuation in underdoped La<sub>2-x</sub>Sr<sub>x</sub>CuO<sub>4</sub>, Nature 406 (2000) 486.
- [11] Y. Wang, L. Li, N.P. Ong, Nernst effect in high-T<sub>c</sub> superconductors, Phys. Rev. B 73 (2006), 024510.
- [12] L. Li, Y. Wang, S. Komiya, S. Ono, Y. Ando, G.D. Gu, N.P. Ong, Diamagnetism and Cooper pairing above T<sub>c</sub> in cuprates, Phys. Rev. B 81 (2010), 054510.
- [13] N.P. Ong, Y. Wang, S. Ono, Y. Ando, S. Uchida, Vorticity and the Nernst effect in cuprate superconductors, Ann. Phys. 13 (2004) 9.
- [14] M.-S. Nam, C. Mézière, P. Batail, L. Zorina, S. Simonov, A. Ardavan, Superconducting fluctuations in organic molecular metals enhanced by Mott criticality, Sci. Rep. 3 (2013), 3390.
- [15] T. Yamashita, Y. Shimoyama, Y. Haga, T.D. Matsuda, E. Yamamoto, Y. Onuki, H. Sumiyoshi, S. Fujimoto, A. Levchenko, T. Shibauchi, Y. Matsuda, Colossal thermomagnetic response in the exotic superconductor URu<sub>2</sub>Si<sub>2</sub>, Nat. Phys. 11 (2015) 17
- [16] V. Khanna, R. Mankowsky, M. Petrich, H. Bromberger, S.A. Cavill, E. Möhr-Vorobeva, D. Nicoletti, Y. Laplace, G.D. Gu, J.P. Hill, M. Först, A. Cavalleri, S. S. Dhesi, Restoring interlayer Josephson coupling in La<sub>1.885</sub>Ba<sub>0.115</sub>CuO<sub>4</sub> by charge transfer melting of stripe order, Phys. Rev. B 93 (2016), 224522.
- [17] W. Hu, S. Kaiser, D. Nicoletti, C.R. Hunt, I. Gierz, M.C. Hoffmann, M. Le Tacon, T. Loew, B. Keimer, A. Cavalleri, Optically enhanced coherent transport in YBa<sub>2</sub>Cu<sub>3</sub>O<sub>6,5</sub> by ultrafast redistribution of interlayer coupling, Nat. Mater. 13 (2014) 705.
- [18] C.R. Hunt, D. Nicoletti, S. Kaiser, D. Pröpper, T. Loew, J. Porras, B. Keimer, A. Cavalleri, Dynamical decoherence of the light induced interlayer coupling in YBa<sub>2</sub>Cu<sub>3</sub>O<sub>6+δ</sub>, Phys. Rev. B 94 (2016), 224303.
- [19] M. Mitrano, A. Cantaluppi, D. Nicoletti, S. Kaiser, A. Perucchi, S. Lupi, P. Di Pietro, D. Pontiroli, M. Riccò, S.R. Clark, D. Jaksch, A. Cavalleri, Possible light-induced superconductivity in K3C60 at high temperature, Nature 530 (2016) 461.
- [20] A. Cantaluppi, M. Buzzi, D. Nicoletti, M. Mitrano, D. Pontiroli, M. Riccò, A. Perucchi, P. Di Pietro, A. Cavalleri, Pressure tuning of light-induced superconductivity in K3C60, Nat. Phys. 14 (2018) 837.
- [21] M. Buzzi, D. Nicoletti, M. Fechner, N. Tancogne-Dejean, M.A. Sentef, A. Georges, T. Biesner, E. Uykur, M. Dressel, A. Henderson, T. Siegrist, J.A. Schlueter, K. Miyagawa, K. Kanoda, M.-S. Nam, A. Ardavan, J. Coulthard, J. Tindall, F. Schlawin, D. Jaksch, A. Cavalleri, Photomolecular high-temperature superconductivity, Phys. Rev. X 10 (2020), 031028.
- [22] A. Dubroka, M. Rössle, K.W. Kim, V.K. Malik, D. Munzar, D.N. Basov, A. A. Schafgans, S.J. Moon, C.T. Lin, D. Haug, V. Hinkov, B. Keimer, T. Wolf, J. G. Storey, J.L. Tallon, C. Bernhard, Evidence of a precursor superconducting phase at temperatures as high as 180K in RBa<sub>2</sub>Cu<sub>3</sub>O<sub>7-δ</sub> (R = Y, Gd, Eu) superconducting crystals from infrared spectroscopy, Phys. Rev. Lett. 106 (2011), 047006.
- [23] T. Timusk, C.C. Homes, The role of magnetism in forming the c-axis spectral peak at 400 cm<sup>-1</sup> in high temperature superconductors, Solid State Commun. 126 (2003) 63.

- [24] T. Moriya, K. Ueda, Antiferromagnetic spin fluctuation and superconductivity, Rep. Prog. Phys. 66 (2003) 1299.
- [25] T. Moriya, K. Ueda, Spin fluctuations and high temperature superconductivity, Adv. Phys. 49 (2000) 555.
- [26] Y.J. Uemura, Muon spin relaxation studies of unconventional superconductors: first-order behavior and comparable spin-charge energy scales, in: A. Avella, F. Mancini (Eds.), Strongly Correlated Systems, Springer series in solid-state sciences, 180, 2015, pp. 237–267, Springer.
- [27] Y.J. Uemura, Energy-scale phenomenology and pairing via resonant spin-charge motion in FeAs, CuO, heavy fermion and other exotic superconductors, Physica B 404 (2009) 3195–3201.
- [28] Y.J. Uemura, A. Keren, L.P. Le, G.M. Luke, W.D. Wu, Y. Kubo, Y. Shimakawa, M. Subramanian, J.L. Cobb, J.T. Markert, Magnetic-field penetration depth in Tl<sub>2</sub>Ba<sub>2</sub>CuO<sub>6+δ</sub> in the overdoped regime, Nature 364 (1993) 605.
- [29] Ch. Niedermayer, C. Bernhard, U. Binninger, H. Glückler, J.L. Tallon, E.J. Ansaldo, J.I. Budnick, Muon spin rotation study of the correlation between Tc and ns/m\* in overdoped Tl<sub>2</sub>Ba<sub>2</sub>CuO<sub>6+δ</sub>, Phys. Rev. Lett. 71 (1993) 1764.
- [30] A. Keren, A. Kanigel, J.S. Lord, A. Amato, Universal superconducting and magnetic properties of the (Ca<sub>x</sub>La<sub>1-x</sub>)(Ba<sub>1.75-x</sub>La<sub>0.25+x</sub>)Cu<sub>3</sub>O<sub>y</sub> system: a μSR investigation, Solid State Commun. 126 (2003) 39.
- [31] I. Božović, X. He, J. Wu, A.T. Bollinger, Dependence of the critical temperature in overdoped copper oxides on superfluid density, Nature 536 (2016) 309.
- [32] Y.J. Uemura, Microscopic phase separation in the overdoped region of high-Tc cuprate superconductors, Solid State Commun. 120 (2001) 347.
- [33] Y. Li, A. Sapkota, P.M. Lozano, Z. Du, H. Li, Z. Wu, A.K. Kundu, R.J. Koch, L. Wu, B. L. Winn, S. Chi, M. Matsuda, M. Frontzek, E.S. Božin, Y. Zhu, I. Božović, A. N. Pasupathy, I.K. Drozdov, K. Fujita, G.D. Gu, I.A. Zaliznyak, Q. Li, J. M. Tranquada, Strongly overdoped La<sub>2−x</sub>Sr<sub>x</sub>CuO<sub>4</sub>: evidence for Josephson-coupled grains of strongly correlated superconductor, Phys. Rev. B 106 (2022), 224515.
- [34] P.W. Phillips, N.E. Hussey, P. Abbamonte, Stranger than metals, Science 377 (2022), eabh4273.
- [35] G. Agnolet, D.F. McQueeney, J.D. Reppy, Kosterlitz-Thouless transition in helium films, Phys. Rev. B 39 (1989), 8934.
- [36] D.J. Bishop, J.E. Berthold, J.M. Parpia, J.D. Reppy, Superfluid density of thin 4He films adsorbed in porous Vicor glass, Phys. Rev. B 24 (1981), 5047.
- [37] H. Chyo, G.A. Williams, Superfluid phase transition of 3He–4He mixture films adsorbed on alumina powder, J. Low Temp. Phys. 110 (1998) 533.
- [38] W. Thomlinson, J.A. Tarvin, L. Passell, Excitations in few-atomic-layer adsorbed helium films: the two-dimensional roton, Phys. Rev. Lett. 44 (1980) 266.
- [39] T.R. Prisk, N.C. Das, S.O. Diallo, G. Ehlers, A.A. Podlesnyak, N. Wada, S. Inagaki, P. E. Sokol, Phases of superfluid helium in smooth cylindrical pores, Phys. Rev. B 88 (2013), 014521.
- [40] E. Blackburn, S.K. Sinha, C. Broholm, J.R.D. Copley, R.W. Erwin, J.M. Goodkind, Neutron scattering study of the excitation spectrum of solid helium at ultra-low temperatures, Pramana; J. Phys. 71 (2008) 673.
- [41] B. Nachumi, A. Keren, K. Kojima, M. Larkin, G.M. Luke, J. Merrin, O. Tchernyshyov, W.D. Wu, Y.J. Uemura, N. Ichikawa, M. Goto, S. Uchida, Muon spin relaxation studies of Zn-substitution effects in high-Tc cuprates, Phys. Rev. Lett. 77 (1996) 5421–5424.
- [42] by Y.J. Uemura, Energy scales of high-Tc cuprates, doped fullerenes, and other exotic superconductors, in: H.C. Ren (Ed.), Proceedings of International Symposium/Workshop on High-Tc Superconductivity and the C60 Family, May 1994, Beijing, Gordon and Breach, New York, 1995, pp. 113–142. by.
- [43] by Y.J. Uemura, Energy scales of exotic superconductors, in: E. Salje, A. S. Alexandrov, Y. Liang (Eds.), Polarons and Bipolarons in High-Tc Superconductors and Related Materials, Cambridge University Press, 1995, pp. 453–460. by.
- [44] S. Wakimoto, K. Ishii, H. Kimura, M. Fujita, G. Dellea, K. Kummer, L. Braicovich, G. Ghiringhelli, L.M. Debeer-Schmitt, G.E. Granroth, High-energy magnetic excitations in overdoped La<sub>2-x</sub>Sr<sub>x</sub>CuO<sub>4</sub> studied by neutron and resonant inelastic x-ray scattering, Phys. Rev. B 91 (2015), 184513.